G. Matthias Ullmann* and Elisa Bombarda

pK_a values and redox potentials of proteins. What do they mean?

Abstract: In this article, we review a microstate model that uses protonation and redox microstates in order to understand the complex pH and redox titration of proteins and other polyelectrolytes. From this model, it becomes obvious that it is impossible to assign pK_a values or redox potentials to individual protonatable or redox-active sites in a protein in which many of such sites interact. Instead each site is associated with many microscopic equilibrium constants that may lead to irregular or even non-monotonic titration curves of some groups. The microstate model provides a closed theoretical framework to discuss such phenomena.

Keywords: microstate model; pH titration; proteins; protonation; redox potentials.

*Corresponding author: G. Matthias Ullmann, Structural Biology/ Bioinformatics, University of Bayreuth, Universitätsstrasse 30, BGI, 95447 Bayreuth, Germany, e-mail: ullmann@uni-bayreuth.de
Elisa Bombarda: Experimental Physics IV, University of Bayreuth, Universitätsstrasse 30, 95447 Bayreuth, Germany

Introduction

Electron and proton transfer reactions and their couplings are central in biochemistry and particularly in bioenergetics (Saraste, 1999; Einsle and Kroneck, 2004). Traditionally, the energetics of these charge transfer reactions is discussed in terms of the pK_a values and redox potentials of the participating groups. However, it is not straightforward to understand the meaning of a pK_a value or a redox potential in a protein. In this minireview, we try to clarify some important issues involved in charge transfer reactions and discuss a microstate model that allows to treat charge transfer reactions in a closed manner.

The protonation and redox equilibria of proteins are interesting for many reasons. The protonation or redox state of a group influences the electrostatic potential of a protein and thus to a great extent also the interaction of this protein with other molecules (Ullmann et al., 2000; Ubbink, 2004). Moreover, these equilibria also influence

the efficiency of enzymatic reactions, charge transfer reactions and protein stability (Antosiewicz and Shugar, 2011; Popovic and Stuchebrukhov, 2012). Often in these cases, the interesting question is not really 'What is the pK_a of this group?', but rather 'How much energy is required to protonate this group?'

The energetics of protonation or redox equilibrium of a functional group in a particular protein can be considerably different from that of the same group in aqueous solution or in another protein. These differences are caused by desolvation effects or local interactions such as hydrogen bonds. Moreover, a protein usually harbors many protonatable or redox active groups. Their mutual interaction makes the theoretical description of charge transfer reactions in proteins more complicated. These equilibria will be analyzed in detail below.

The energetics of protonation and redox reactions

A protonation equilibrium of a single protonatable group can be described by Eq. (1), where K_a is the equilibrium constant:

$$\mathrm{HA} \underset{}{\overset{K_a}{\rightleftharpoons}} \mathrm{A^-} + \mathrm{H^+}; \quad K_a = \frac{[\mathrm{A^-}][\mathrm{H^+}]}{[\mathrm{HA}]} \tag{1}$$
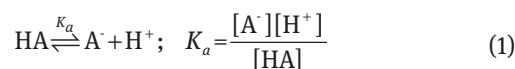
The pK_a of an acid and the pH of the solution are respectively defined as the negative decadic logarithm of the K_a value (pK_a=-lgK_a) and of the activity of the hydrogen ions (pH=-lgγ[H⁺], where γ is the activity coefficient and [H⁺] is the proton concentration in the bulk solution). With these definitions we obtain the Henderson-Hasselbalch equation [Eq. (2)] from Eq. (1):

$$\mathrm{pH} = \mathrm{p}K_a + \lg \frac{[\mathrm{A^-}]}{[\mathrm{HA}]} \tag{2}$$

The pK_a value relates to the standard reaction free energy $G^{\circ}_{\mathrm{prot}}$ as given by $G^{\circ}_{\mathrm{prot}} = -RT \ln 10\, \mathrm{p}K_a$, where R is the gas

constant and T the absolute temperature. The free energy G_{prot} required to protonate a titratable group at a given pH and temperature is given by Eq. (3):

$$G_{\text{prot}} = -RT \ln 10 \, (\, \text{p}K_a\text{-pH}\,) = G_{\text{prot}}^{\text{o}} - \mu_{\text{H}^+} \tag{3}$$

Importantly, the energetics of the protonation reaction can be defined through the chemical potential of protons μ_{H^+} as the second part of Eq. (3) shows. From Eq. (3), it can also be seen that a pK_a value at a given temperature can be considered as a unitless energy. The definition of the pH value is mainly historical. Discussions of titration curves in terms of pH values are sometimes a bit counterintuitive because a low pH value implies a high proton concentration (or actual activity) and *vice versa*. A discussion of titration curves in terms of chemical potentials removes this problem.

Redox equilibrium can be described equivalently. The equilibrium between the redox couple $A_{\text{ox}}/A_{\text{red}}^-$ is defined as:

$$A_{\text{ox}} + e^- \overset{K_{ET}}{\rightleftharpoons} A_{\text{red}}^-; \quad K_{ET} = \frac{[\,A_{\text{red}}^-\,]}{[\,A_{\text{ox}}\,][\,e^-\,]} \tag{4}$$

where K_{ET} is the equilibrium constant. Analogously to the pH and pK_a, we define the solution redox potential E (or the electrode potential) and the midpoint potential E^{o} of the redox couple $A_{\text{ox}}/A_{\text{red}}^-$ as $E = -RT/F\ln[e^-]$ and $E^{\text{o}} = RT/F\ln K_{ET}$, respectively. Here, however, the natural logarithm rather than the decadic logarithm is used. With factor RT/F, where F is the Faraday constant, we obtain E and E^{o} in volts. The relation between E^{o} and the standard reaction free energy $G_{\text{redox}}^{\text{o}}$ is given by $G_{\text{redox}}^{\text{o}} = FE^{\text{o}}$. With these definitions and Eq. (4), we obtain the Nernst equation [Eq. (5)]:

$$E = E^{\text{o}} + \frac{RT}{F}\ln\frac{[\,A_{\text{ox}}\,]}{[\,A_{\text{red}}^-\,]} \tag{5}$$

which is analogous to the Henderson-Hasselbalch equation [Eq. (2)]. The free energy G_{redox} required to reduce a redox-active group (i.e., binding an electron) at a given redox potential of solution E is given by:

$$G_{\text{redox}} = F(\,E\text{-}E^{\text{o}}\,) = G_{\text{redox}}^{\text{o}} - \mu_{e^-} \tag{6}$$

Eq. (6) shows that also for redox reactions, a discussion in terms of chemical potentials is straightforward. One advantage to discussing protonation and redox reactions in terms of chemical potentials instead of pH and redox potentials is that the discussion of these binding reactions can be extended to any kind of binding, such as ion or drug binding (Ullmann and Ullmann, 2012; Ullmann et al., 2012).

From what has been said so far, it can be seen that the theoretical treatment of protonation equilibria and redox equilibria is fully equivalent.

Multiple site titration

The titration curves of a single titratable group are easy to understand. As Figure 1A shows, there are two protonation states that can convert into each other. The sum of the probabilities of the two states is always 1.

When there are two interacting protonatable groups, the situation is more complicated because of the different protonation states (microstates) involved in the process. A molecule with two interacting sites has four possible microstates: fully protonated, protonated at one group, protonated at the other group, and fully unprotonated (Figure 1B). These states can be described by their protonation state vectors: (11), (10), (01) and (00), where 1 and 0 mark that the corresponding group is protonated or deprotonated, respectively. In order to obtain the titration curve of one group, the probabilities of the microstates in which this group is protonated need to be added. For instance, the titration curve of group one is given by $\langle x_1 \rangle = \langle 10 \rangle + \langle 11 \rangle$. The titration curves of such groups can considerably deviate from standard sigmoidal titration curves and can show highly irregular features because of electrostatic interactions between the titrating groups. The assignment of a pK_a value to one particular group in such cases is difficult if not impossible. The same is true for redox potential in the case of molecules with several interacting redox-active groups. To eliminate the difficulties, the problem can be reformulated. Instead of considering a protein as a system of groups with a certain protonation probability, the problem can be formulated in terms of well-defined microstates of the protein that have a certain probability of occurrence, as will be outlined now.

Let us consider a system that possesses N protonatable sites and K redox-active sites. Such a system can adopt $M = 2^{N+K}$ states assuming that each site can exist in two forms. The interaction between them can be modeled purely electrostatically, i.e., the electronic coupling is negligible. Each state of the system can be written as an $N+K$-dimensional vector $\vec{x} = (x_1, \cdots, x_{N+K})$, where x_i is 0 or 1 if site i is deprotonated (reduced) or protonated (oxidized), respectively. Each state of the system has a well-defined energy that depends on the energetics of the individual sites and the interaction between sites. The energy of a state $\vec{x}_v$ is given by (Bashford and Karplus, 1990; Ullmann and Knapp, 1999; Ullmann, 2000; Nielsen and McCammon, 2003; Gunner et al., 2006):
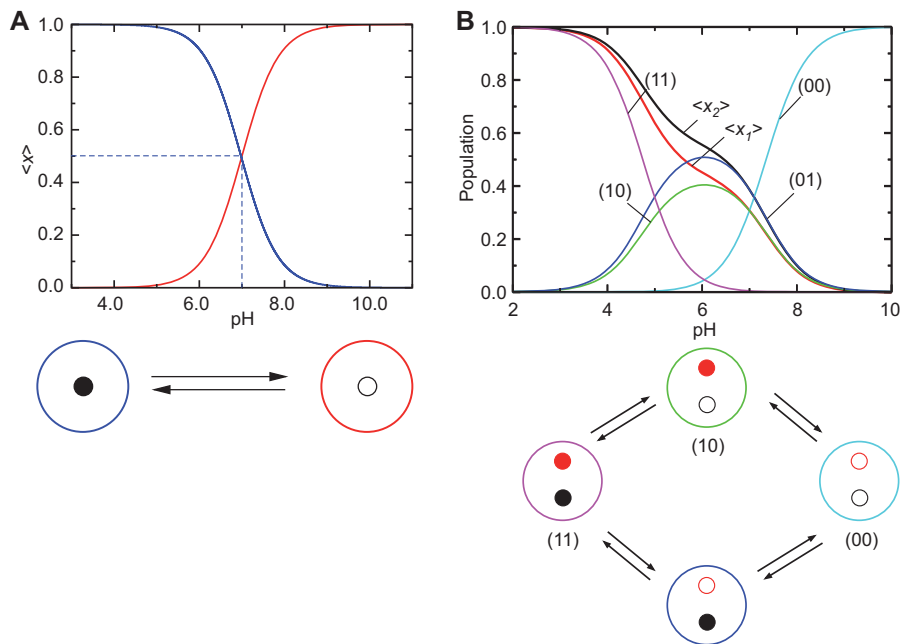
Figure 1 Titration behavior of molecules with one and two protonatable groups. (A) Titration curve of an acid with one titratable group. The titration curve has a sigmoidal shape. (B) Titration curve of an acid with two titratable groups. The contributions of the population of the different microstates lead to non-sigmoidal titration curves. The microstates and their populations, the titration curves and the sites are color coded in the reaction scheme and in the diagram. The titration curve of the red site is the sum of the probability of the magenta microstate population curve of state (11) and the green microstate the population curve of state (10).

$$G(\vec{x}_\nu) = \sum_{i=1}^{N}(x_{\nu,i}-x_i^\circ)RT\ln10\,(\,\mathrm{pH}-\mathrm{p}K_{a,i}^{\mathrm{intr}}\,)$$
$$-\sum_{i=1}^{K}(x_{\nu,i}-x_i^\circ)F(E-E_i^{\mathrm{intr}}) \tag{7}$$
$$+\frac{1}{2}\sum_{i=1}^{N+K}\sum_{j=1}^{N+K}(x_{\nu,i}-x_i^\circ)(x_{\nu,j}-x_j^\circ)W_{ij}$$

where R is the gas constant; T is the absolute temperature; F is the Faraday constant; $x_{\nu,i}$ denotes the protonation or redox form of the site i in state $\vec{x}_\nu$; x_i° is the reference form of site i; p$K_{a,i}^{\mathrm{intr}}$ and E_i^{intr} are the pK_a value and redox potential, respectively, that site i would have if all other sites are in their reference form (intrinsic pK_a value and intrinsic redox potential); E is the reduction potential of the solution; pH is the pH value of the solution; and W_{ij} represents the interaction of site i with site j.

The equilibrium properties of a physical system are completely determined by the energies of its states. To keep the notation concise, states will be numbered by Greek indices, i.e., for state energies we write G_ν instead of $G(\vec{x}_\nu)$. For site indices, the roman letters i and j will be used. The equilibrium probability of a single state $\vec{x}_\nu$ is given by:

$$P_\nu^{eq} = \frac{e^{-\beta G_\nu}}{Z} \tag{8}$$

with $\beta=1/RT$ and Z being the partition function of the system.

$$Z = \sum_{\nu=1}^{M}e^{-\beta G_\nu} \tag{9}$$

The sum runs over all M possible states. Properties of single sites can be obtained from Eq. (8) by summing up the individual contributions of all states. For example, the probability of site i being protonated is given by:

$$\langle x_i\rangle = \sum_{\nu}^{M}x_{\nu,i}P_\nu^{eq} \tag{10}$$

where $x_{\nu,i}$ denotes the protonation form of site i in the charge state $\vec{x}_\nu$. For small systems, this sum can be evaluated explicitly. For larger systems, Monte-Carlo techniques can be used to determine these probabilities (Beroza et al., 1991; Ullmann and Ullmann, 2012).

The energetic parameters p$K_{a,i}^{\mathrm{intr}}$ and E_i^{intr} are calculated as shifts of the deprotonation or reduction energy

compared to its value for an appropriate model compound in aqueous solution.

$$pK_{a,i}^{intr} = pK_a^{model} - \frac{1}{RT\ln 10}(\Delta\Delta G_i^{Born} + \Delta\Delta G_i^{back}) \qquad (11)$$

$$E_i^{intr} = E_{model}^{o} - \frac{1}{F}(\Delta\Delta G_i^{Born} + \Delta\Delta G_i^{back}) \qquad (12)$$

where pK_a^{model} and E_{model}^{o} are the pK_a value or redox potential of an appropriate model compound. For instance, a model compound for a glutamate residue in a protein would be the N-acetylated and C-amidated glutamate. $\Delta\Delta G_i^{Born}$ is the shift of the deprotonation or reduction energy due to a change in the solvation energy. This term usually destabilizes the charged form inside the protein, since an amino acid is better solvated in the solvent than inside the protein. $\Delta\Delta G_i^{back}$ is the energy shift due to interaction with non-titrating charges and dipoles inside the protein. These energy shifts as well as the interaction energy W_{ij} between two groups can be calculated on the basis of the Poisson-Boltzmann equation (Bashford and Karplus, 1990; Ullmann and Knapp, 1999).

For a system of interacting sites, the protonation or reduction probabilities $\langle x_i \rangle$ can show a complex shape, thus rendering the assignment of pK_a values or mid-point potentials to individual sites difficult or even meaningless (Onufriev et al., 2001; Ullmann, 2003, 2004; Onufriev and Ullmann, 2004; Klingen et al., 2006). In contrast, the energy differences between microstates remain well defined and thus provide a convenient basis to describe the system. For individual sites in such a complex system, we can however define pH-dependent pK_a values and solution redox potential dependent midpoint potentials (Bombarda and Ullmann, 2010).

$$pK_i = pH + \frac{1}{\ln 10}\left(\ln\frac{\langle x_i \rangle}{1-\langle x_i \rangle}\right) \qquad (13)$$

$$E_i^{o} = E + \frac{RT}{F}\left(\ln\frac{\langle x_i \rangle}{1-\langle x_i \rangle}\right) \qquad (14)$$

These values define properties that are directly related to a free energy difference (Bombarda and Ullmann, 2010) and are relevant for understanding enzymatic mechanisms.

The formalism described here is applicable only to sites that have two states, i.e., either protonated and deprotonated or oxidized and reduced. For some sites, such as those in flavins or quinones, the situation is more complicated because these molecules exist in multiple redox and protonation states. For such cases, the formalism needs to

be extended (Ullmann and Ullmann, 2012). The equations become slightly more complicated, nevertheless the basic philosophy stays the same and the microstate model can be applied.

Some illustrative examples

Two interacting sites that titrate in the same pH range

Figure 2 shows the titration behavior of a molecule with two strongly interacting sites. The strength of the interaction between the sites can be read from the difference between the microscopic pK_a values associated with the same site (Figure 2A). In case there would be no interaction, the pK_a values for deprotonating the same site are the same. The stronger the interaction, the greater the difference between the microscopic pK_a values associated with the deprotonation of the same site. In this example, the interaction energy is equivalent to 2 pH units (which is equal to approximately 2.8 kcal/mol). The titration curves (Figure 2B) deviate from a standard sigmoidal shape and it is not very surprising that we cannot describe the titration curve with a standard pK_a value. Using a rearranged Henderson-Hasselbalch equation [Eq. (13)], we can see that the pK_a values that are assigned to the sites depend on the pH and converge to the microscopic pK_a values at the extreme pH values (Figure 2C).

Figure 2D shows the pH dependence of the protonation energy. The straight lines (dotted-dashed lines in Figure 2D) describe the pH dependence of the protonation energy of one group while the other group stays in the same protonation state, which corresponds to the transitions between microstates, as shown in Figure 2A. The protonation energy of the individual groups does not depend linearly on pH as would be the case for an isolated protonatable group. Instead, the protonation energy is close to zero over the relatively wide pH range in which the groups titrate.

Two interacting sites that titrate in different pH ranges

At a first sight, the situation seems to be more straightforward if we consider a system in which the titratable groups do not titrate in the same pH range. Figure 3 shows a situation in which two groups interact strongly (as above, the interaction is about 2 pH units, Figure 3A). Their titration
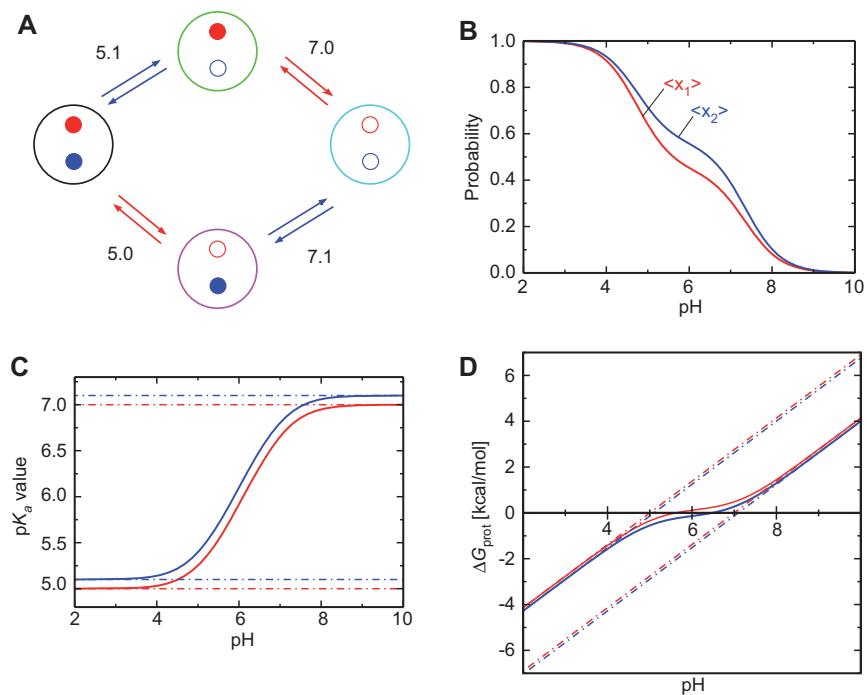
Figure 2 Titration curve of two sites that titrate in the same pH range. (A) Equilibria with microscopic pK_a values; (B) non-sigmoidal titration curves of the system; (C) pH-dependent pK_a values calculated from the titration curves using equation 13. The solid lines give the pH-dependent pK_a values. The dotted-dashed lines show the microscopic pK_a values. (D) Protonation energy as a function of pH. The solid lines give the protonation energies of the individual sites. The dotted-dashed lines show the protonation energies of the microstates.
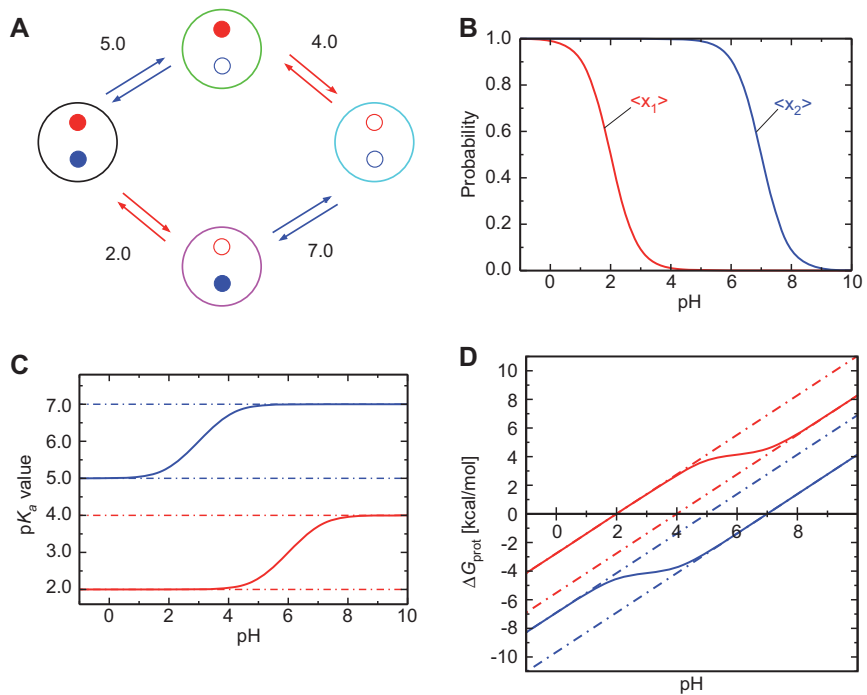

Figure 3 Titration curve of two sites that titrate in different pH ranges. (A) Equilibria with microscopic pK_a values; (B) Sigmoidal titration curves of the system; (C) pH-dependent pK_a values calculated from the titration curves using equation 13. The solid lines give the pH-dependent pK_a values. The dotted-dashed lines show the microscopic pK_a values. (D) Protonation energy as a function of pH. The solid lines give the protonation energies of the individual sites. The dotted-dashed lines show the protonation energies of the microstates.

curves seem to have a normal sigmoidal shape (Figure 3B) and from these titration curves we are tempted to assign a pK_a of 2 to the first group and a pK_a of 7 to the second group. However, a closer analysis shows that for such a system we also have to define several microscopic pK_a values. At low pH, group two would show a pK_a of 5 and only at higher pH, i.e., when group one is already deprotonated, group two shows a pK_a of 7 (Figure 3C). The transition from a pK_a of 5 to a pK_a of 7 occurs in the pH range where group one changes its protonation. Similarly for group two, we find a pK_a of 2 at low pH, when group one is still protonated and a pK_a of 4 at high pH. The transition from a pK_a of 2 to a pK_a of 4 occurs in the pH range where group two changes its protonation. The protonation energy of group one is nearly constant over the pH range when group two changes its protonation and *vice versa* (Figure 3D).

In pure equilibrium situations, group one would never show a pK_a of 4 and group two would never show a pK_a of 5. However, in non-equilibrium situations as may occur during catalysis, group one may act as a proton donor with a pK_a of 4 and group two may act as a proton acceptor with a pK_a of 5. These microscopic pK_a values may not show up as features in the titration curves since the population of the relevant microstates is below the detection limit. Nevertheless, these microstates may be of functional importance and can be relevant for possible reaction mechanisms.

Diethylenetriamine pentaacetate: a molecule with unusual experimental titration curves

Titration curves with a non-sigmoidal shape can be seen in many protein titration studies, and their interpretation is often very complicated. However, small molecules may also show a complex titration behavior. One example is diethylenetriamine pentaacetate (DTPA; Figure 4A). This molecule has three amine groups: two terminal amines and one central amine. Each of theses groups can bind a proton. In the fully stretched conformation, the distance between the terminal nitrogen atoms is about 7.5 Å and about 3.8 Å between the terminal nitrogen atom and the central nitrogen atom. The individual titration curves have been measured by nuclear magnetic resonance (Kula and Sawyer, 1964; Sudmeier and Reilley, 1964; Letkeman, 1979). Using the individual titration curves, it is possible for DTPA to determine microscopic pK_a values (Figure 4B) and from them it is possible to obtain the population probabilities of the microscopic protonation states in dependence on pH (Onufriev et al., 2001; Ullmann, 2003). Figure 4C and D show the individual

titration curves and the population of all states that contribute to the titration of the terminal amines and the central amine, respectively. Since the molecule is symmetric, the titration curves of the two terminal amines are identical.

The titration curve of the central amine is unusual because of its non-monotonic shape. In particular, between pH 7 and pH 10 the probability of protonation increases with increasing pH (i.e., with decreasing proton concentration). The population of the microstates gives a physical reason for the unusual, irregular titration behavior of the central amine of DTPA. At high pH (low proton concentration), the protons preferentially bind to the central amine, because the binding affinity of a proton to the middle nitrogen is higher. Binding of the second proton to one of the terminal amines while the central amine stays protonated is unfavorable, because these two proton binding sites are in close proximity and the positively charged protons repel each other. Therefore, when the second proton binds, it is more favorable to deprotonate the central amine and to protonate both terminal amines. When the two terminal amines are protonated, the two protons are at a greater distance from each other, and thus they repel each other less than if one terminal and the central amine are protonated. Finally, at very low pH (high proton concentration) all three sites will bind a proton.

Obviously, it is not easy to assign pK_a values to the individual sites. The terminal amines are associated with four microscopic pK_a values and the central amine with three, because the microstates (110) and (011) are indistinguishable (Figure 4B and 4D). (However, using equation 13 it is possible to assign an effective pK_a value to each site (Figure 4E). It can be seen that the effective pK_a value varies within the limits of the microscopic pK_a values.

Even more interesting than the pH-dependence of the pK_a values is the pH-dependence of the protonation energy. For isolated titratable groups, the pK_a value is pH independent and the protonation energy depends linearly on pH. In the case of non-isolated titratable groups like in DTPA, the pK_a value is pH-dependent and consequently the pH-dependence of the protonation free energy becomes non-linear. Figure 4F shows the pH-dependent protonation free energy of DTPA. Interestingly, the protonation energy of the sites of DTPA is nearly pH-independent over a large pH range. Thus, the central amine group can function as a proton donor or acceptor over a large pH range.

Even if DTPA seems to be an extreme example, similarly complicated protonation equilibria caused by charge-charge interactions frequently occur in proteins
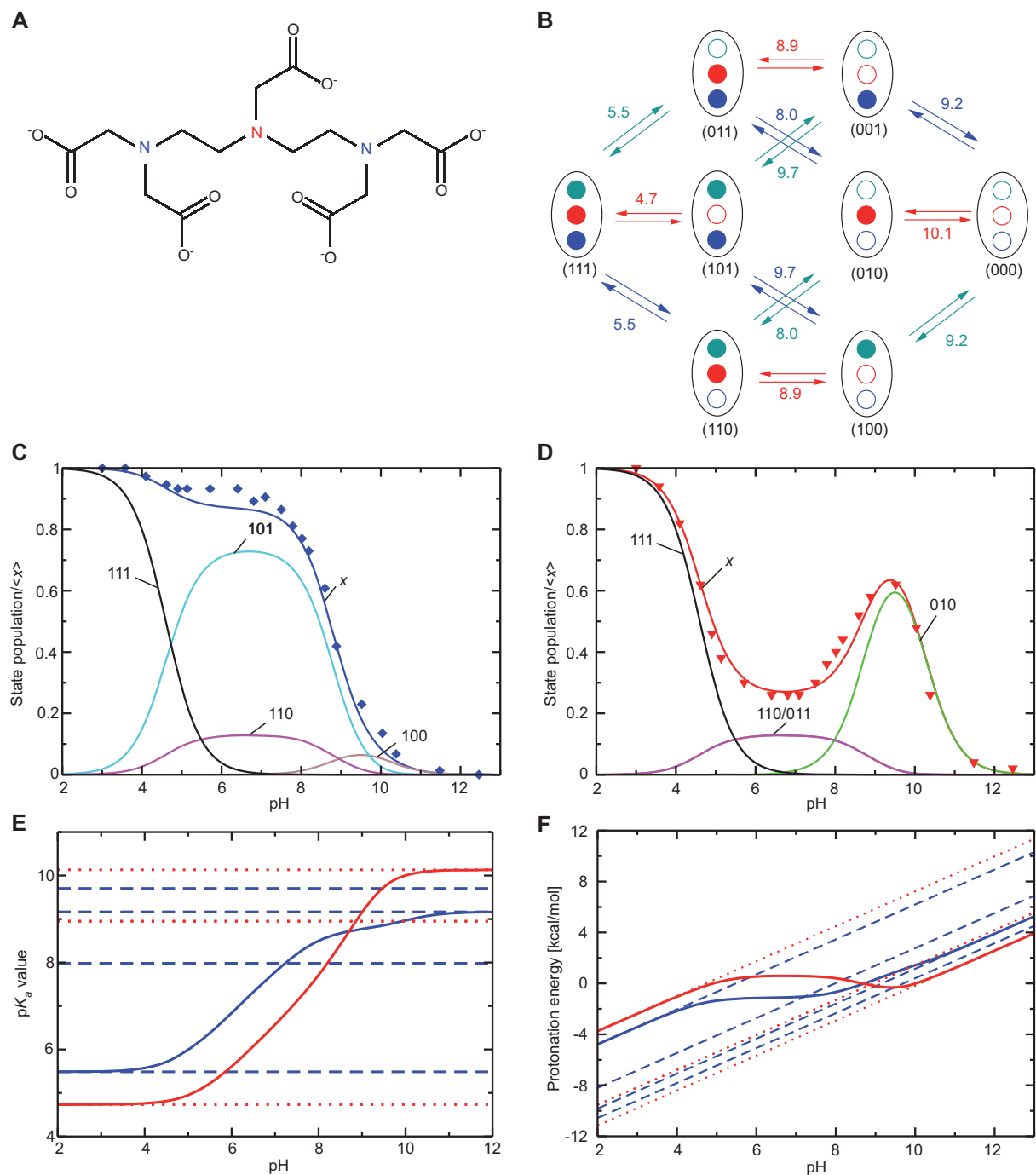
Figure 4 Titration behavior of diethylenetriamine pentaacetate (DTPA). (A) Structural formula of DTPA at basic pH. The titrating amines are shown in red (central nitrogen) and blue (terminal nitrogens). Since the molecule is symmetrical, the left and right terminal amines behave equivalently. In the fully stretched conformation, the distance between the terminal nitrogen atoms is about 7.5 Å and is about 3.8 Å between the terminal nitrogen atom and the central nitrogen atom. (B) Microscopic protonation equilibria. The numbers at the arrows indicate the microscopic pK_a values. (C) Titration curve of the terminal amines together with the population of the states that are contributing to this titration curve. (D) Titration curve of the central amine together with the population of the states that are contributing to this titration curve. (E) pH-dependent effective pK_a values (solid lines) and microscopic pK_a values (dashed and dotted lines). (F) pH-dependent effective protonation energies (solid lines) and microscopic protonation energies (dashed and dotted lines).

as discussed in previous papers (Klingen et al., 2006; Ullmann and Ullmann, 2011). Irregular titration curves are a sign of such complications. Furthermore, even if the titration curves in proteins apparently show a standard sigmoidal shape, the interactions between titratable groups can cause pH-dependent pK_a values (Bombarda and Ullmann, 2010). Such pH-dependent pK_a values may lead to nearly pH-independent protonation energies in a certain pH range and thus may explain why some particular residue can function as proton donor or acceptor over a large pH range allowing catalysis under different pH conditions. Probably for this reason, there are often more protonatable residues in the active site of enzymes than the specific function would require.

Conclusion and outlook

We have shown in this review how the complex titration behavior of proteins can be understood in a consistent way with the use of a microstate model. According to this model, we cannot assign a single pK_a value (or redox potential) to a titratable group in a protein. Instead we assume that each titratable group can exist in two states, for instance protonated or deprotonated and oxidized or reduced, leading to 2^N possible states for a protein with N titratable groups. We can define $N2^{N-1}$ microscopic equilibrium constants of which only 2^N-1 are independent of each other (Ullmann, 2003). The titration of a protein can be discussed in terms of these microscopic pK_a values and all apparent conflicts, such as irregular or even non-monotonic titration curves, can be resolved.

The microstate model can also be applied in the discussion of reaction mechanisms and even in the simulation of the kinetics of such mechanisms using a master equation approach (Becker et al., 2007). By applying the master equation to the re-reduction electron transfer of the special pair in the reaction center from *Blastochloris viridis*, we were able to consistently reproduce experimental kinetic data that were not previously understood and we showed that neglecting interaction between charge transfer partners leads to incorrect results (Bombarda and Ullmann, 2011). Thus, the concept of microscopic constants is essential for the analysis of a complex charge transfer reaction, no matter whether the reactions are electron transfer, proton transfer or coupled.

We can conclude that the determination of pK_a values and redox potentials in a protein is a difficult task, even experimentally. Theoretical calculations using continuum electrostatics are able to predict the pK_a values, redox potentials, and titration curves of sites in proteins assuming that all possible conformations of the protein are taken into consideration. This method normally produces good results for active site residues in stable conformations for which the understanding of the titration behavior is most interesting (Taly et al., 2003; Calimet and Ullmann, 2004; Bombarda et al., 2006; Kim et al., 2005; Song and Gunner, 2009; Zhang and Gunner, 2010), even if it may fail to predict the right titration behavior at pH values outside the stability range of the protein.

In our opinion, an understanding of complex charge transfer reactions without a detailed theoretical analysis is impossible. The microstate model that we have discussed in this review and that we have implemented in an extended form in our GMCT software (Ullmann and Ullmann, 2012) provides a sound basis for such a theoretical analysis.

References

Antosiewicz, J.M. and Shugar, D. (2011). Poisson-Boltzmann continuum-solvation models: applications to pH-dependent properties of biomolecules. Mol. BioSyst. *7*, 2923–2949.

Bashford, D. and Karplus, M. (1990). pKas of ionizable groups in proteins: Atomic detail from a continuum electrostatic model. Biochemistry *29*, 10219–10225.

Becker, T., Ullmann, R.T., and Ullmann, G.M. (2007). Simulation of the electron transfer between the tetraheme-subunit and the special pair of the photosynthetic reaction center using a microstate description. J. Phys. Chem. B *111*, 2957–2968.

Beroza, P., Fredkin, D.R., Okamura, M.Y., and Feher, G. (1991). Protonation of interacting residues in a protein by a Monte

Carlo method: application to lysozyme and the photosynthetic reaction center. Proc. Natl. Acad. Sci. USA *88*, 5804–5808.

Bombarda, E. and Ullmann, G.M. (2010). pH-dependent pK_a values in proteins – A theoretical analysis of protonation energies with practical consequences for enzymatic reactions. J. Phys. Chem. B *114*, 1994–2003.

Bombarda, E. and Ullmann, G.M. (2011). Continuum electrostatic investigations of charge transfer processes in biological molecules using a microstate description. Faraday Discuss. *148*, 173–193.

Bombarda, E., Becker, T., and Ullmann, G.M. (2006). The influence of the membrane potential on the protonation of bacteriorhodopsin:

insights from electrostatic calculations into the regulation of proton pumping. J. Am. Chem. Soc. *128*, 12129–12139.

Calimet, N. and Ullmann, G.M. (2004). The influence of a transmembrane pH gradient on protonation probabilities of bacteriorhodopsin: the sructural basis of the back-pressure effect. J. Mol. Biol. *339*, 571–589.

Einsle, O. and Kroneck, P. (2004). Structural basis of denitrification. Biol. Chem. *385*, 875–883.

Gunner, M.R., Mao, J., Song, Y., and Kim, J. (2006). Factors influencing the energetics of electron and proton transfers in proteins. What can be learned from calculations. Biochim. Biophys. Acta, *1757*, 942–968.

Kim, J., Mao, J., and Gunner, M.R. (2005). Are acidic and basic groups in buried proteins predicted to be ionized? J. Mol. Biol. *348*, 1283–1298.

Klingen, A.R., Bombarda, E., and Ullmann, G.M. (2006). Theoretical investigation of the behavior of titratable groups in proteins. Photochem. Photobiol. Sci. *5*, 588–596.

Kula, R. and Sawyer, D. (1964). Protonation studies of anion of diethylenetriaminepentaacetic acid by nuclear magnetic resonance. Inorg. Chem. *3*, 458.

Letkeman, P. (1979). An NMR protonation study of metal diethylene-triaminepentaacetic acid complexes. J. Chem. Ed. *56*, 348–351.

Nielsen, J.E. and McCammon, J.A. (2003). Calculating pKa values in enzyme active sites. Protein Sci. *12*, 1894–1901.

Onufriev, A. and Ullmann, G.M. (2004). Decomposing complex ligand binding into simple components: connections between microscopic and macroscopic models. J. Phys. Chem. B *108*, 11157–11169.

Onufriev, A., Case, D.A., and Ullmann, G.M. (2001). A novel view on the pH titration of biomolecules. Biochemistry *40*, 3413–3419.

Popovic, D.M. and Stuchebrukhov, A.A. (2012). Coupled electron and proton transfer reactions during the O – E transition in bovine cytochrome c oxidase. Biochim. Biophys. Acta-Bioenerg. *1817*, 506–517.

Saraste, M. (1999). Oxidative phosphorylation at the fin de siecle. Science *121*, 1488–1493.

Song, Y.F. and Gunner, M.R. (2009). Using multiconformation continuum electrostatics to compare chloride binding motifs in alpha-amylase, human serum albumin, and Omp32. J. Mol. Biol. *387*, 840–856.

Sudmeier, J.L. and Reilley, C.N. (1964). Nuclear magnetic resonance studies of protonation of polyamine and aminocar-boxylate compounds in aqueous solution. Analyt. Chem. *36*, 1698–1706.

Taly, A., Sebban, P., Smith, J.C., and Ullmann, G.M. (2003). The structural changes in the Q_B pocket of the photosynthetic reaction center depend on pH: a theoretical analysis of the proton uptake upon Q_B reduction. Biophys. J. *84*, 2090–2098.

Ubbink, M. (2004). Complexes of photosynthetic redox proteins studied by NMR. Photosyn. Res. *81*, 277–287.

Ullmann, G.M. (2000). The coupling of protonation and reduction in proteins with multiple redox centers: theory, computational method, and application to cytochrome c_3. J. Phys. Chem. B *104*, 6293–6301.

Ullmann, G.M. (2003). Relations between protonation constants and titration curves in polyprotic acids: a critical view. J. Phys. Chem. B *107*, 1263–1271.

Ullmann, G.M. and Knapp, E.W. (1999). Electrostatic computations of protonation and redox equilibria in proteins. Eur. Biophys. J. *28*, 533–551.

Ullmann, R.T. and Ullmann, G.M. (2011). Coupling of protonation, reduction, and conformational change in azurin from Pseudomonas aeruginosa investigated with free energy measures of cooperativity. J. Phys. Chem. B *115*, 10346–10359.

Ullmann, R.T. and Ullmann, G.M. (2012). GMCT: a Monte Carlo Simulation package for macromolecular receptors. J. Comp. Chem. *33*, 887–900.

Ullmann, G.M., Hauswald, M., Jensen, A., and Knapp, E.W. (2000). Superposition of ferredoxin and flavodoxin using their electrostatic potentials. Implications for their interactions with photosystem I and ferredoxin:NADP reductase. Proteins *38*, 301–309.

Ullmann, R.T., Andrade, S.L.A., and Ullmann, G.M. (2012). Thermo-dynamics of transport through the ammonium transporter amt-1 investigated with free energy calculations. J. Phys. Chem. B *116*, 9690–9703.

Zhang, J. and Gunner, M.R. (2010). Multiconformation continuum electrostatics analysis of the effects of a buried Asp introduced near He me a in Rhodobacter sphaeroides cytochrome c oxidase. Biochemistry *49*, 8043–8052.